

# Conservativeness of untied auto-encoders

Anonymous Author(s)

Affiliation

Address

email

## Abstract

We discuss necessary and sufficient conditions for an autoencoder to define a conservative vector field, in which case it is associated with an energy function akin to the unnormalized log-probability of the data. We show that, contrary to the common folklore, the conditions for conservativeness are more general than for encoder and decoder weights to be the same (“tied weights”) and they also depend on the form of the hidden unit activation function. We also show that contractive training criteria, such as denoising regularization, will automatically enforce these conditions locally, near the mode of the data density.

## 1 Introduction

An autoencoder is a feature learning model that learn to reconstruct its inputs by going through one or more capacity-constrained “bottleneck”-layers. Since it defines a mapping from  $r(\mathbf{x}) : \mathbb{R}^n \rightarrow \mathbb{R}^n$ , an autoencoder can also be viewed as dynamical system, that is trained to have fixed points at the data [8]. Recent renewed interest in the dynamical systems perspective led to a variety of new results that help clarify the role of autoencoders and their relationship to probabilistic models. For example, [10, 9] showed that training an autoencoder to denoise corrupted inputs is closely related to performing score matching [5] in an undirected model. Similarly, [1] showed that training the model to denoise inputs, or to reconstruct them under a suitable choice of regularization penalty, lets the autoencoder approximate the derivative of the empirical data density. And [6] showed that, regardless of training criterion, any autoencoder whose weights are tied (decoder-weights are identical to the encoder weights) can be written as the derivative of a scalar “potential-” or energy-function, which in turn can be viewed as unnormalized data log-probability. For sigmoid hidden units the potential function is exactly identical to the free energy of an RBM, which shows that there is tight link between these two types of model.

The same is not true for untied autoencoders, for which it has not been clear whether such an energy function exists. It has also not been clear under which conditions an energy function exists or does not exist, or even how to define it in the case where decoder-weights differ from encoder weights. In this paper, we describe necessary and sufficient conditions for the existence of an energy function and we show that suitable learning criteria will lead to an autoencoder that satisfies these conditions at least locally, near the training data. We verify our results experimentally. We also show how we can use an autoencoder to extract the conservative part from a vector field.

## 2 Background

We will focus on auto-encoders of the form

$$r(\mathbf{x}) = Rh(W^T \mathbf{x} + \mathbf{b}) + \mathbf{c} \quad (1)$$

where  $\mathbf{x} \in \mathbb{R}^n$  is an observation,  $R$  and  $W$  are decoder and encoder weights, respectively, and  $\mathbf{b}$  and  $\mathbf{c}$  are biases. An autoencoder can be identified with its vector field,  $r(\mathbf{x}) - \mathbf{x}$ , which is the set of

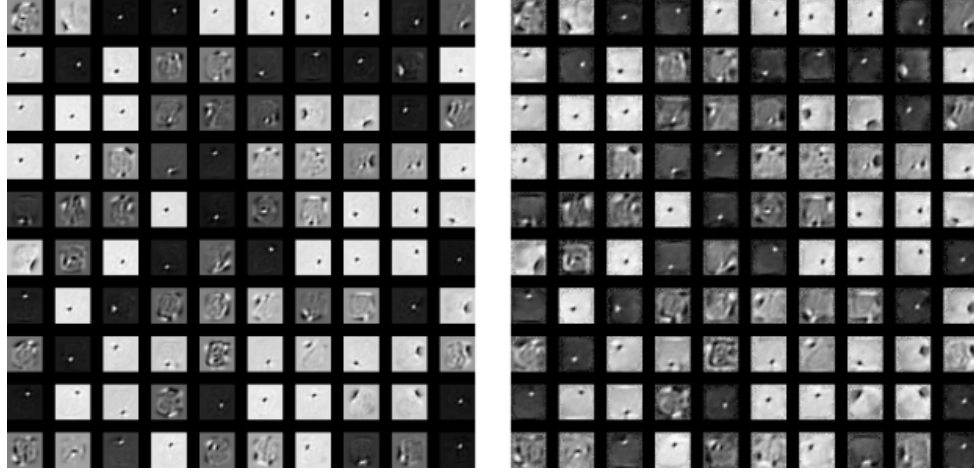


Figure 1: Figure presents the weights of encoder  $W$  (Left) and weights of decoder  $R^T$  (Right). Two weights are highly identical to each other.

vectors pointing from observations to their reconstructions under the autoencoder. The vector field is called conservative if it can be written as the gradient of a scalar function  $F(\mathbf{x})$ , called potential or energy function:

$$r(\mathbf{x}) - \mathbf{x} = \nabla F(\mathbf{x}) \quad (2)$$

In this case, we can integrate the vector field to find the potential energy [6], which for tied weights and real-valued observations takes the general form

$$F(\mathbf{x}) = \int h(\mathbf{u}) d\mathbf{u} - \frac{1}{2} \|\mathbf{x} - \mathbf{c}\|_2^2 + \text{const} \quad (3)$$

where  $\mathbf{u} = W^T \mathbf{x} + \mathbf{b}$  is an auxiliary variable and  $h(\cdot)$  can be any elementwise activation function with known anti-derivative of its function. For example, the energy function of an autoencoder with sigmoid activation function is identical to the (Gaussian) RBM free energy [4]:

$$F_{\text{sig}}(\mathbf{x}) = \sum_k \log(1 + \exp(W_{\cdot k}^T \mathbf{x} + b_k)) - \frac{1}{2} \|\mathbf{x} - \mathbf{c}\|_2^2 + \text{const} \quad (4)$$

A sufficient condition for the existence of an energy function is that the weights are tied [6], but it has not been clear if this is also necessary. A peculiar phenomenon in practice is that it is very common for decoder and encoder weights to be “similar” (albeit not necessarily tied) in response to training. An example of this effect is shown in Figure 1. This raises the question why this happens, and whether the quasi-tying of weights has anything to do with the emergence of an energy function, and if yes, whether there is a way to compute the energy function despite the lack of exact symmetry. We shall address these questions in what follows.

### 3 Conservative auto-encoders

One in of the central objective of this paper is understanding the conditions for an autoencoder to be conservative<sup>1</sup> and have a well-defined potential energy function. In the following subsection we derive and explain said conditions.

#### 3.1 Conditions for the conservative auto-encoders

**Proposition 1.** Consider a  $m$ -hidden-layer auto-encoder defined as

$$r(\mathbf{x}; \theta) = R h^{(m)} \left( h^{(k)} \dots h^{(1)}(\mathbf{x}) \right) + \mathbf{b}^{(m)},$$

<sup>1</sup>The expressions, “conservative vector field” and “conservative autoencoders” will be used interchangeably.

where  $\theta = \cup_{k=0}^m \theta^{(k)}$  such that  $\theta^{(k)} = \{W^{(k)}, R^{(k)}, \mathbf{b}^{(k)}\}$  are the parameters of the model, and  $h^{(k)}(\cdot)$  is a smooth elementwise activation function at layer  $k$ . Then the auto-encoder is said to be conservative over a smooth simply connect domain  $K \subseteq \mathbf{R}^D$  if and only if its reconstruction's Jacobian  $\frac{\partial r(\mathbf{x})}{\partial \mathbf{x}}$  is symmetric for all  $x \in K$ .

A formal proof is provided in the supplementary material.

A region  $K$  is said to be *simply connected* if and only if any simple curve in  $K$  can be shrunk to a point. It is not always the case that a region of  $\mathbf{R}^D$  is simply connected. For instance, a curve surrounding a punctured circle in  $\mathbf{R}^2$  cannot be continuously deformed to a point without crossing the punctured region. However, as long as we make the reasonable assumption that the activation function does not have a continuum of discontinuities, we should not run into trouble. This makes our analysis valid for activation functions with cusps such as *relu*.

Throughout the paper our focus will be on one-hidden-layer auto-encoders. Although the necessary and sufficient conditions for their conservativeness are a special case of the above proposition, it is worth deriving them explicitly.

**Proposition 2.** Let  $r(x)$  be a one-hidden-layer autoencoder with  $D$  dimensional inputs and  $H$  hidden units,

$$r(\mathbf{x}) = Rh(W^T \mathbf{x} + \mathbf{b}) + \mathbf{c},$$

where  $R, W, \mathbf{b}, \mathbf{c}$  are the parameters of the model. Then  $r(x)$  defines a conservative vector field over a smooth simply connect domain  $K \subseteq \mathbf{R}^D$  if and only if  $RD_{h'}W^T$  is symmetric for all  $x \in K$  where  $D_{h'} = \text{diag}(h'(\mathbf{x}))$ .

*Proof.* Following proposition 1, an autoencoder defines a conservative vector field if and if its Jacobian is symmetric for all  $x \in K$ .

$$(\forall x \in K) \frac{\partial r(\mathbf{x})}{\partial \mathbf{x}} - \left( \frac{\partial r(\mathbf{x})}{\partial \mathbf{x}} \right)^T = 0 \quad (5)$$

By explicitly calculating the Jacobian, this is equivalent to

$$(\forall x \in K) (\forall 1 \leq i < j \leq D) \sum_{l=0}^H (R_{jl}W_{li} - R_{il}W_{lj})h'_l(\mathbf{x}) = 0 \quad (6)$$

Defining  $D_{h'} = \text{diag}(h'(\mathbf{x}))$ , this hold if and only if

$$(\forall x \in K) RD_{h'}W^T = WD_{h'}R^T \quad (7)$$

□

For tied weights, one-hidden-layer autoencoders in Equation 7 becomes automatically symmetric regardless of what the choice of activation function  $h$  and  $\mathbf{x}$  is.

**Corollary 0.1.** An autoencoder with tied weights always defines a conservative vector field.

Proposition 2 illustrates that one-layered tied autoencoders are actually a subset of the set of all conservative one-layered autoencoders. Moreover, the inclusion is strict. That is to say there are untied conservative autoencoders that are not trivially equivalent to tied ones. As example, let us compare the parametrization of tied and conservative untied linear one-layered autoencoders.  $r_{\text{untied}}(x)$  defines a conservative vector field if and only  $RW^T = WR^T$  which offers a richer parametrization than the tied linear autoencoder  $r_{\text{tied}}(x) = WW^T x$ .

### 3.2 Understanding the symmetricity condition

Remark that if symmetricity in the Jacobian of auto-encoder's reconstruction function, then the vector field is conservative. Now, we turn our interest to discussing some of the sufficient conditions that leads to symmetricity in the Jacobian of auto-encoder's reconstruction function.

For the existence of a potential energy function for 1-layer auto-encoder is to have symmetric matrices from left and right of  $WD_{h'}$  such that

$$R = CWD_{h'}E. \quad (8)$$

where  $C$  and  $E$  are symmetric matrices, and  $C$  commutes with  $WD_{h'}ED_{h'}W^T$ . This is due to the symmetry of the partial derivatives being satisfied when the decoder weights are defined by  $R = CWD_{h'}E$  where  $C$  and  $E$  are symmetric matrices, and  $C$  commutes with  $WD_{h'}ED_{h'}W^T$ :

$$\frac{\partial \mathbf{r}(\mathbf{x})}{\partial \mathbf{x}} = RD_{h'}W^T = CWD_{h'}ED_{h'}W^T = WD_{h'}ED_{h'}W^TC = WD_{h'}R^T = \left( \frac{\partial \mathbf{r}(\mathbf{x})}{\partial \mathbf{x}} \right)^T.$$

Thus, the vector field must be conservative.

In the case of a symmetric auto-encoder where  $R = W$ , the matrix  $E$  becomes

$$E = \text{diag} \left( h' \left( W^T \mathbf{x} \right) \right)^{-1} \quad (9)$$

and  $C$  becomes identity, which will let us have  $\frac{\partial \mathbf{r}(\mathbf{x})}{\partial \mathbf{x}} = RD_{h'}W^T = WD_{h'}^{-1}D_{h'}W^T = WW^T$ .

Notice that  $R = CWD_{h'}$  and  $R = WD_{h'}E$  are the special case of the  $R = CWD_{h'}E$  when  $E$  is an identity for the first case and  $C$  is an identity for the latter case. Moreover, we can also find a matrix  $E$  and  $C$  given the parameters  $W$  and  $R$ , which are presented in Section 1.2 of the supplementary material.

We can try to understand the role of symmetric matrix  $C$  through the lens of spectral decomposition. Remark that two symmetric matrix are commutative if they lie on the same eigen space, i.e. they have same eigenvectors. Then,

$$CWD_{h'}D_{h'}W^T = Q\Lambda Q^T Q\Sigma Q^T = Q\Lambda\Sigma Q^T \quad (10)$$

where  $Q\Lambda Q^T$  is the eigen decomposition of  $C$  and  $Q\Sigma Q^T$  is the eigen decomposition of  $WD_{h'}D_{h'}W^T$ . This illustrates that one can simply find  $C$  based on choosing a  $\Lambda$ , and  $\Lambda$  merely stretches or shrinks along the direction of eigenvectors. Additionally, the role of  $E$  in  $R = WD_{h'}E$  can be explained as scaling the pre-activation of the hidden units when  $E$  is the diagonal matrix. This can be directly observed re-expressing the condition in terms of elementwise operations, then

$$R_{jl} = W_{jl}E_{ll} \forall l = 1 \cdots H, \forall j = 1 \cdots D. \quad (11)$$

Hence, the filters  $R_{.l}$  gets brightened or dimmed depending on the diagonal matrix of  $E_{ll}$ .

## 4 Explaining the Symmetricity

Now that we have established the conditions for conservativeness, We focus on understanding why does auto-encoders desire to become symmetric during the training.

We proceed in two steps in order to explain, the apparently unexpected, weights symmetry of trained autoencoders.

We start by considering the local behaviour of trained contractive autoencoders around the fixed points under the ideal condition of knowing the data true distribution. Next, we proceed to analyze the symmetricity of empirically trained autoencoders.

### 4.1 Autoencoders Dynamics around Fixed Points

Let  $r(\mathbf{x})$  be an autoencoder that minimizes the squared loss function of the true data distribution,

$$L_\sigma(\mathbf{x}) = \int_{\mathbb{R}^d} \left[ \|r(\mathbf{x}) - \mathbf{x}\|_2^2 + \sigma^2 \left\| \frac{\partial r(\mathbf{x})}{\partial \mathbf{x}} \right\|_2^2 \right] d\mathbf{x} \quad (12)$$

A point  $\bar{\mathbf{x}} \in \mathbb{R}^d$  is a fixed point of  $r(\mathbf{x})$  if and only if  $r(\bar{\mathbf{x}}) = \bar{\mathbf{x}}$ . We will drop the bar in the following to avoid cluttering the notation.

Taking a first order Taylor expansion of  $r(\mathbf{x})$  around  $\mathbf{x}$  yields

$$r(\mathbf{x} + \epsilon) = \mathbf{x} + \frac{\partial r(\mathbf{x})}{\partial \mathbf{x}}^T \epsilon^2 + o(\epsilon^2) \text{ as } \epsilon \rightarrow 0 \quad (13)$$

[2] shows that the reconstruction  $r(\mathbf{x}) - \mathbf{x}$  becomes an estimator of the score when it is small and the contraction parameters  $\epsilon \rightarrow 0$ . Hence around a fixed point we have

$$r(\mathbf{x} + \epsilon) - \mathbf{x} = \epsilon \frac{\partial \log(p(\mathbf{x}))}{\partial \mathbf{x}} \quad (14)$$

Which implies that,

$$\frac{\partial(r(\mathbf{x} + \epsilon) - \mathbf{x})}{\partial \mathbf{x}} = I + \epsilon \frac{\partial^2 \log(p(\mathbf{x}))}{\partial \mathbf{x}^2} \quad (15)$$

Where  $I$  is the identity matrix.

Explicitly expressing the Jacobian of the autoencoder's dynamics  $\frac{\partial r(\mathbf{x}) - \mathbf{x}}{\partial \mathbf{x}}$  and combining the Taylor expansion of  $r(\mathbf{x})$ , the Equation 15 yields to

$$W^T D_{h'} A^T - I = \epsilon \frac{\partial^2 \log(p(\mathbf{x}))}{\partial \mathbf{x}^2} \quad (16)$$

The Hessian of  $\log p(\mathbf{x})$  being symmetric by construction, the Equation 16 illustrates that around fixed points,  $AD_{h'}W$  is symmetric and hence, by *Proposition 2*,  $r(\mathbf{x}) - \mathbf{x}$  is conservative.

Another way to understand and gain intuition about the dynamics of a trained encoder is to consider it as a dynamical system [6].

Using the typical linearization argument, dynamics around fixed points can be understood by analyzing the eigenvalues of the Jacobian. The latter being symmetric implies that its eigenvalues cannot have complex parts. This in turn explains the lack of oscillations one would naturally expect of a conservative vector field. Moreover, in directions orthogonal to the fixed point, the eigenvalues of the reconstruction will be negative. Thus the fixed point is actually a sink.

## 4.2 Conservativeness near the data concentrated modes

Based on our theoretical results, we can only talk about auto-encoder's conservativeness only if the auto-encoder is well-trained, in which

$$\frac{\partial r(\mathbf{x})}{\partial \mathbf{x}} = \left( \frac{\partial r(\mathbf{x})}{\partial \mathbf{x}} \right)^T. \quad (17)$$

This naturally impose the conservativity to auto-encoder's vector field. Therefore, here, we analyze whether the Equation 17 is satisfied as the model is trained, and if not, what can we do to enforce this constraints.

Fortunately, in practice, we recognized that the weights of auto-encoders become akin to one and other (Figure 1). First, we measured the symmetricity using  $\text{sym}(A) = \frac{\|(A+A^T)/2\|^2}{\|A\|^2}$  where the range of symmetricity function lies between  $[0, 1]$  and symmetricity value will approach to 1 as the matrix  $A$  becomes more symmetric. The symmetric auto-encoders will be always trivially zero. For untied auto-encoders, Figure 2a and 2c shows the symmetricity curve of  $\frac{\partial r(\mathbf{x})}{\partial \mathbf{x}} = RD_{h'}W$  during the training. We trained an untied auto-encoder with 500 hidden units and with (and without) weight constraints on MNIST dataset. For non-symmetric auto-encoders, we observe that they tend to become symmetric as the training proceeds. As expected, the contractive auto-encoder conduces more towards being symmetry than regular auto-encoder. AE and CAE reaches plateau around 0.951 and 0.974 respectively.

Table 1: Symmetricity of ADW after training AEs with 500 units on MNIST for 100 epochs. We denote the auto-encoders with weight length constraints as '+wl'.

	Relu	Relu+wl	sig.+wl	sig.+wl
AE	95.9%	98.7%	95.1%	99.1%
CAE	95.2%	98.6%	97.4%	99.1%

Interestingly, we recognized that the auto-encoder with weight length constraints give

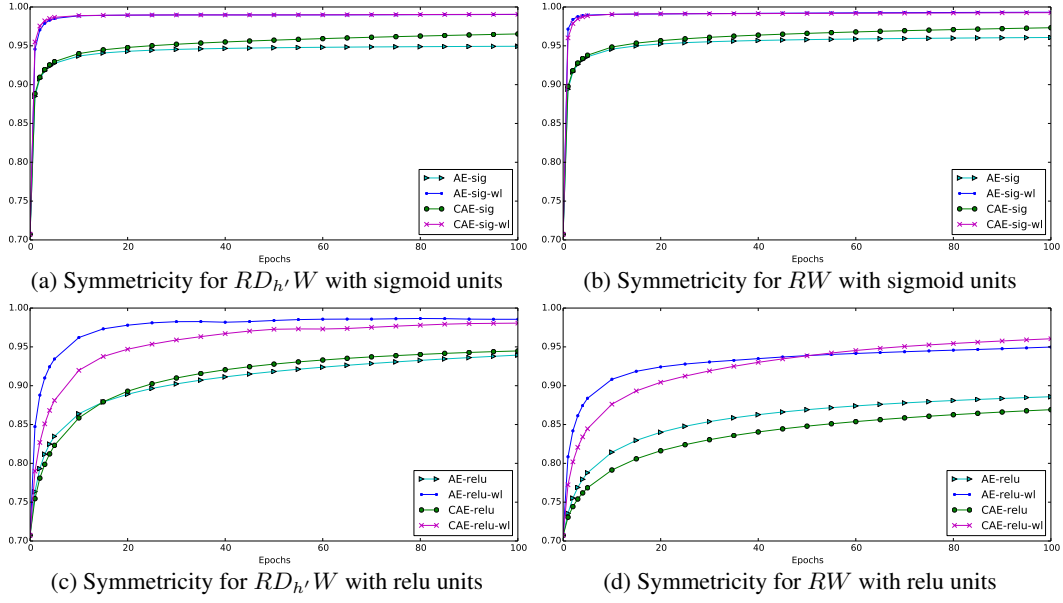


Figure 2: The symmetry distance of  $\frac{\partial r(\mathbf{x})}{\partial \mathbf{x}}$  and the symmetry distance of  $RW^T$  for sigmoid activation and relu activation are illustrated over the learning time of the auto-encoder.

much higher score on the symmetry of Jacobians as shown in Table 1. We report the details of the experiments and reasonings in the supplementary material.

Additionally, we studied auto-encoders with different activation function. Though, we have seen that auto-encoder becomes symmetric for sigmoid<sup>2</sup> and relu activation function, another intriguing notice was that we observe symmetry in  $RW^T$  for sigmoid but not for relu activation function as shown in Figure 2b and 2d. This implies that the activations of sigmoid hidden units, at least for training data points, are independent of  $h'(\mathbf{x})$ . Although, both (sigmoid and relu) auto-encoder becomes symmetric, the symmetry curves behave utterly differently on  $RW^T$ .

Deeper analysis using the following equation explains the different behaviour:

$$\sum_{l=1}^H (R_{il}W_{lj} - R_{jl}W_{li})h'_l(\mathbf{x}) = 0, \forall 1 \leq i, j \leq d \quad (18)$$

In the case of sigmoid with weight length constraints,  $RW^T \simeq WR^T$ . We notice that most of the hidden units lie on the highest curvature region due to the weight length constraints<sup>3</sup>. This enforces  $h_l(\mathbf{x})$  to be concentrated on high curvature regions of sigmoid activation and most of hidden units seem to lie on the region where  $h'_l(\mathbf{x})$  is linear. These observations lead to two cases:

1.  $h'_l(\mathbf{x})$  are constant for all  $l$  given  $\mathbf{x}$
2.  $h'_l(\mathbf{x})$  are linear independent.

In practice, it is hard to examine which one of the cases is more likely to happen, but both of the cases will make  $RW^T = WR^T$  since  $\sum_l (R_{il}W_{lj} - R_{jl}W_{li}) = 0$  for the first case and  $(R_{il}W_{lj} - R_{jl}W_{li}) = 0$  for the second case in Equation 18. Thus,  $RW^T = WR^T$ . Similarly, sigmoid auto-encoder with no weight constraints is highly symmetric, but not as ones with weight constraints, possibly due to the vanishing  $h'_l(\mathbf{x})$  for some  $l$ s. On the other hand, the presence of linear and zero function in relu activation makes Equation 18 behave much differently. We can define a set of hidden units that are active and not active such that the units belong to the active set if  $W^T x > 0$  and

<sup>2</sup>This happens for any kinds of sigmoid function like logistic and tanh function.

<sup>3</sup>The histogram of hidden activation units are shown in the supplementary material.

otherwise they belong to inactive set. Considering just the active set,  $h'_l(\mathbf{x}) = 1$  by the definition of relu, which makes  $\sum_{l=1}^S (R_{il}W_{lj} - R_{jl}W_{li}) = 0$  where  $S$  is the active hidden units. In the case of non active set,  $h'_l(\mathbf{x}) = 0$ , which will automatically satisfy the Equation 18 without satisfying  $RW^T = WR^T$ . One may also be curious about deeper layers of auto-encoder. We also provide a symmetricity curve for 2-layer auto-encoder in the supplementary material and it shows that they still desires to be symmetric as well.

Besides providing symmetricity curve, we also explicitly show that auto-encoder is becoming more conservative by presenting magnitude of curl curve on the various 2D synthetic dataset. They are presented on the supplementary materials.

## 5 Decomposing the Vector Field

In this section, we will consider finding the closest conservative vector field, in the last square sense, to a non-conservative field. Before diving into the algorithm, it is worth mentioning that many communities such as fluid mechanics, physics, and computer graphic and vision have developed various ways to decompose the vector fields into an irrotational and a solenoidal fields.

### 5.1 The Helmholtz-Hodge decomposition

To motivate the idea, let's first discuss from the perspective of exterior calculus. The fundamental theorem of vector calculus, also known as Helmholtz decomposition [], states that any vector field can be expressed as the sum of an irrotational and a solenoidal field. Furthermore, extending from  $\mathbb{R}^3$  to differential forms on a Riemannian manifold, the Hodge Helmholtz decomposition of any arbitrary  $k$ -form in terms of a  $k - 1$ -form,  $k + 1$  form and a harmonic  $k$ -form:

$$\omega = d\alpha + \delta\beta + \gamma \quad (19)$$

where  $d$  is the exterior derivative,  $\delta$  the co-differential, and  $\Delta\gamma = 0$ . This means that any vector field can be decomposed into scalar(symmetric), solenoidal (anti-symmetric tensor), and harmonic (rotational) vector fields and they are orthogonal to each other.

This shows that it is always possible, in theory, to get the orthogonal projection of the 1-form implied by the autoencoder on the space of all exact 1-forms. In the language of vector fields, it is always possible to find the closest conservative vector field, in the least square sense, to a non-conservative vector fields. This guarantees the existence of a best approximate energy function, again in the least square sense, for any autoencoder. Moreover, the Hodge decomposition in Equation 19 is constructive in the sense that it formally characterizes the components and the inner product definition.

### 5.2 Learning to approximate the conservative vector field

Here, we take the approach where we leverage another model to learn the non-conservative vector field using tied and untied-auto-encoders. This approach has several advantages as follows: i) The key advantage of using tied auto-encoders is that learning the scalar vector field component  $\alpha$  from some vector field  $\omega$  is straightforward due to their intrinsic properties of tied weights or  $\frac{\partial r(\mathbf{x})}{\partial \mathbf{x}}$  desiring to become symmetric. ii) There has been many works that explicitly computes the projections, however, these methods have the downside, where the boundary conditions interplays key role in their formulation of the decomposition. Whereas, the formulation of statistical learning based methods does not depend on boundary condition. iii) Additionally, given the expressiveness of neural network (including auto-encoders), they ought to be compatible with other statistical learning based methods such as matrix-valued radial basis function kernel[7].

In our experiments, we constructed set of vector fields  $\mathcal{F} = \{F_0, F_1, \dots, F_K\}$  based on interpolating the two vector fields  $F_0$  and  $F_K$ .  $F_0$  is a non-conservative vector field which is defined by an untied auto-encoder with the random weights  $(W_0, R_0)$  such that  $R_0W_0^T$  is not symmetric.  $F_K$  is a conservative vector field

---

**Algorithm 1** Learning to approximate conservative field using auto-encoders

---

- 1: **procedure** ( $\mathcal{D}$  be a data set )
- 2:   Let  $(W_0, R_0)$  be a random weights for AE.
- 3:   Let  $(W_K, R_K)$  be trained AE on  $\mathcal{D}$ .
- 4:   Generate  $F_i \forall i = 1 \dots K$  as follows:
  - $(W_i, R_i) = \beta(W_0, R_0) + (1 - \beta)(W_K, R_K)$
  - Sample  $\mathbf{x}_i$  from uniform distribution in the data space.
  - $\mathcal{F}_i = \{(\mathbf{x}_i, r(\mathbf{x}_i)) \text{ for } i = 1 \dots N\}$
- 5:   **for** each vector field  $F_i$ , **do**
- 6:     Train a tied Auto-encoder on  $F_i$

which is defined by tied (untied)<sup>4</sup> auto-encoder and this auto-encoder was trained using MNIST dataset.  $F_k$ s are the vector fields which were created by interpolating the weights  $(W_0, R_0)$  and  $(W_K, R_K)$  based on following formulation:  $(W_i, R_i) = \beta(W_0, R_0) + (1 - \beta)(W_K, R_K)$ . We created the vector field dataset  $\mathcal{D}_{F_i}$  by generating vectors  $(\mathbf{x}_k, r(\mathbf{x}_k))$  where half of the  $\mathbf{x}_k$ s were from MNIST dataset and another half was randomly sampled points from the bionomial distribution, so that our vector field dataset is not just focused on the data manifold but over the all space. Using these datasets, we trained tied auto-encoders to learn the conservative vector fields.

Next, we examine whether the model was able to approximate the conservative component of the vector field through two implicit testing. First way to verify that the auto-encoder does learn the conservative component is to observe the status of training cost (mean square error). The auto-encoder should be able to minimize its cost lower as the  $\beta$  approaches to 1, i.e. as the dataset becomes more conservative. Indeed, this is what we find. Figure 5.2 shows the mean square error plot while training the vector fields data for different  $\beta$ . We see that as  $\beta$  approaches from 0.0 to 1.0, auto-encoder was able to minimize its objective function closer to 0.0.

In order to evaluate the experiment quantitatively, we compared the (unnormalized) likelihood of auto-encoder generating two points at a time where these two points are from the MNIST dataset and corrupted MNIST data using salt and pepper noise. The comparison was based on computing the potential energy of auto-encoders and we validate our experiments based on counting  $\mathbb{1}[E(\mathbf{x}) > E(\mathbf{x}_{\text{rand}})]$  where  $\mathbb{1}$  is the indicator function. Though one can say that the energy at data points should be higher than non-data points for  $(W_k, R_k)$  since the weights are based on training on MNIST dataset, but because we are not using  $(W_k, R_k)$  to compute the energy but to train the tied auto-encoder to predict the vector field created by  $(W_k, R_k)$ , we can conclude that tied auto-encoder was able to learn the conservative vector field. Algorithm 1.

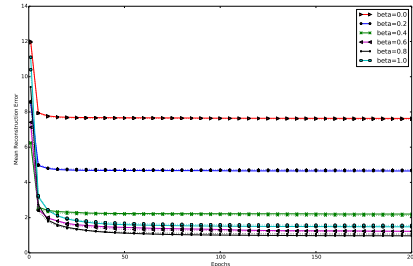


Figure 3: Figure presents objective function (mean reconstruction error) of auto-encoder while training vector fields data on tied (dash) and untied (solid) auto-encoder.

Table 2: The results are normalized score of  $\mathbb{1}[E(\mathbf{x}) > E(\mathbf{x}_{\text{rand}})]$  for different  $\beta$  values.

$\beta$	0.0	0.2	0.4	0.6	0.8	1.0
CVF=Tied AE	0.5036	0.7357	0.9338	0.98838	0.9960	0.9968
CVF=Untied AE	0.5072	0.7496	0.9373	0.98595	0.9958	0.9968

In the ideal scenario, as the vector field  $F_i$  approaches from 0 to  $K$ , we would see the increase in favoring the data points than non-data points. Indeed, Table 2 illustrates that our hypothesis is correct. “CVF=Tied AE” refers to conservative vector field  $F_K$  trained by tied auto-encoder and “CVF=Untied AE” refers to conservative vector field  $F_K$  trained by untied auto-encoder.

## 6 Discussion

The fact that the weights in an autoencoder make it locally conservative in response to suitable training criteria means that inference in the autoencoder by running its dynamics amounts to climbing

<sup>4</sup>We experimented with both tied and untied auto-encoder for  $F_K$  since tied auto-encoder automatically formulates conservative vector field and untied auto-encoder is also empirically shown to be desiring conservativeness when training using mean reconstruction error. In fact, comparing these two experiments and seeing that the results of two experiments are identical, again verifies that untied auto-encoder likes to be conservative.



the energy function. This in turn could be a prerequisite for back-propagating error derivatives and to perform globally consistent updates using local learning rules [3]. An interesting direction for future research includes the parameterization of the autoencoder such that a sufficient condition other than weight tying will be satisfied. Another direction is the use of annealed importance sampling or similar sampling-based approaches to globally couple the local energy function values obtained from untied autoencoders.

## References

- [1] Guillaume Alain and Yoshua Bengio. What regularized auto-encoders learn from the data generating distribution. In *International Conference on Learning Representations*, 2014.
- [2] Guillaume Alain, Yoshua Bengio, Li Yao, Jason Yosinski, Eric Thibodeau-Laufer, Saizheng Zhang, and Pascal Vincent. What regularized auto-encoders learn from the data generating distribution. In <http://arxiv.org/pdf/1503.05571v2.pdf>, 2015.
- [3] Yoshua Bengio, Dong-Hyun Lee, Jorg Bornschein, and Zhouhan Lin. Towards biologically plausible deep learning. *arXiv preprint arXiv:1502.04156*, 2015.
- [4] G. Hinton. A practical guide to training restricted boltzmann machines, version 1. *Momentum*, 9, 2010.
- [5] A. Hyvärinen. Estimation of non-normalized statistical models by score matching. *Journal of Machine Learning Research*, 6, December 2005.
- [6] Hanna Kamyshanska. On autoencoder scoring. In *Proceedings of the International Conference on Machine Learning (ICML)*, pages 720–728, 2013.
- [7] Ives Macedo and Renner Castro. Numerical solution of the navier-stokes equations. In *Technical report*, 2008.
- [8] H. Sebastian Seung. Learning continuous attractors in recurrent networks. In *Proceedings of the Neural Information Processing Systems (NIPS)*, pages 654–660, 1998.
- [9] K. Swersky, D. Buchman, B.M. Marlin, and N. de Freitas. On autoencoders and score matching for energy based models. In *International Conference on Machine Learning (ICML)*, 2011.
- [10] Pascal Vincent, Hugo Larochelle, Yoshua Bengio, and P.A. Manzagol. Extracting and composing robust features with denoising autoencoders. In *Proceedings of the 25th International Conference on Machine Learning (ICML)*, 2008.

---

# Supplementary Material for “On the potential energy of an auto-encoder with untied weights”

---

Anonymous Author(s)

Affiliation

Address

email

In this supplementary material, we presents some background materials, derivations, and supporting explanations that can advocate our presentation is the original paper.

## 1 Conservative untied auto-encoders

A sufficient condition for the auto-encoder to have an energy function states that if  $R = CW$  such that  $C$  is symmetric and commutes with  $WW^T$ , then the auto-encoder’s vector field is conservative. The reason for this is as follows: ...

### 1.1 Towards Poincare’s criterion for untied AE using differential forms

This section provides detailed derivations of the **TODO:Proposition** that is presented in the original paper in Section3.

**Proposition 1.** 2 Consider an auto-encoder that is defined by

$$r(\mathbf{x}; \theta) = Rh(h \cdots h(\mathbf{x})) + \mathbf{c},$$

where  $\theta$  is the parameters of the model, and  $h(\cdot)$  is an elementwise activation function. Then the auto-encoder is said to be conservative if and only if the Jacobian of auto-encoder’s reconstruction function,  $\frac{\partial r(\mathbf{x})}{\partial \mathbf{x}}$ .

The high level idea is that simply solving the anit-derivative of auto-encoder’s vector field as proceeded in [1] does not work for untied auto-encoders. This is due to the difference in solving first order ordinary differential equations for tied auto-encoders and first order partial differntial equations for untied auto-encoders. Therefore, here we present a more elegant approach, where we adopt the differential forms to faciliate the derivation of the existence condition of a potential energy function in the case of untied autoe-encoders.

The advantage of differential forms is that it allows us to work with generalized viewpoint, i.e. free coordinate system. A differntial form  $\alpha$  of degree  $l$  ( $l$ -form) on a smooth domain  $K \subseteq \mathbb{R}^d$  is an expression:

$$\alpha = \sum_{i=1}^D f_i dx_i. \quad (1)$$

Using differential form algebra and exterior derivatives, we can show that 1-form implied by untied auto-encoder is exact, which means that  $\alpha$  can be expresseed as  $\alpha = d\beta$  for some  $\beta \in \Lambda^{l-1}(K)$ . Let  $\alpha$  be the 1-form implied by vector field of untied auto-encoder. Then, we have

$$\alpha = \sum_{i=1}^D r_i dx_i, \text{ and } d\alpha = \sum_{i=1}^D d(r_i \wedge dx_i) \quad (2)$$

where  $\wedge$  is the exterior multiplication,  $d$  is the differential operation on diffrenetial forms, and  $r(\cdot)$  is the reconstruction function of auto-encoder. Based on the rule of exterior derviative properties, i)if  $f \in \Lambda^0(K)$  then  $df = \sum_{i=1}^D \frac{\partial f}{\partial x_i} dx_i$  and ii) if  $\alpha \in \Lambda^l(K)$  and  $\beta \in \Lambda^m(K)$  then  $\alpha\beta = (-1)^{lm}\beta\alpha$ ,

$$d\alpha = \sum_{i=1}^D d(r_i \wedge dx_i) \quad (3)$$

$$= \sum_{i,j=1}^D \frac{\partial r_i}{\partial x_j} (dx_j \wedge dx_i) \quad (4)$$

$$= - \sum_{1 \leq i < j < D} \frac{\partial r_i}{\partial x_j} dx_i \wedge dx_j + \sum_{1 \leq i < j < D} \frac{\partial r_j}{\partial x_i} dx_i \wedge dx_j \quad (5)$$

$$= \sum_{1 \leq i < j < D} \left( \frac{\partial r_i}{\partial x_j} - \frac{\partial r_j}{\partial x_i} \right) dx_i \wedge dx_j \quad (6)$$

According to the Poincare's theorem, which states that every exact form is closed and convrsely, if  $\alpha$  is closed then it is exact in a simply connected region and  $\alpha \in \Lambda^l(K)$ , where  $\alpha$  is closed if  $d\alpha = 0$ . Then, by Poincare's theorem, we see that

$$d\alpha = \sum_{1 \leq i < j < D} \left( \frac{\partial r_i}{\partial x_j} - \frac{\partial r_j}{\partial x_i} \right) dx_i \wedge dx_j = 0 \quad (7)$$

Re-formulating this in terms of  $\frac{\partial r_i}{\partial x_j} = \sum_{l=1}^{dh} A_{il} W_{lj} h'_l(\mathbf{x})$ , we see that

$$\sum_{l=1}^H (R_{jl} W_{li} - R_{il} W_{lj}) h'_l(\mathbf{x}) = 0 \quad (8)$$

for all  $1 \leq i, j < D$  and for all  $\mathbf{x}$ .

## 1.2 Relations between the sufficient conditions

Let's re-state the two sufficient conditions:

1. If  $R = C\hat{W}$  such that  $C$  is symmetric and commutes with  $WW^T$ , then the auto-encoder's vector field is conservative.
2. If  $R = \hat{W}E$  such that  $E$  is diagonal matrix, then the auto-encoder's vector field is conservative.

Now, we find  $C$  and  $E$  given the parameters  $W$  and  $R$ . If  $R = C\hat{W}$  such that  $C$  is symmetric and commutes with  $\hat{W}\hat{W}^T$ , then we know that  $R\hat{W}^T = \hat{W}R^T$ . Then, we can find  $C$  as follows:

$$\begin{aligned} R\hat{W}^T &= \hat{W}R^T \\ C\hat{W}\hat{W}^T &= \hat{W}R^T \\ C &= \hat{W}R^T A^T (AA^T)^{-1} \end{aligned}$$

where  $A = \hat{W}\hat{W}^T$  and  $A^T(AA^T)^{-1}$  is pseudoinverse from the rightside. Similarly, we can also compute  $E$  as shown.

$$\begin{aligned} R\hat{W}^T &= \hat{W}R^T \\ \hat{W}E\hat{W}^T &= \hat{W}R^T \\ E &= (\hat{W}^T \hat{W})^{-1} \hat{W}^T \hat{W} R^T \hat{W} (\hat{W}^T \hat{W})^{-1} \\ E &= R^T \hat{W} (\hat{W}^T \hat{W})^{-1} \end{aligned}$$

since  $(W^T W)^{-1} W^T W = I$ .

## 2 Explaining the symmetry

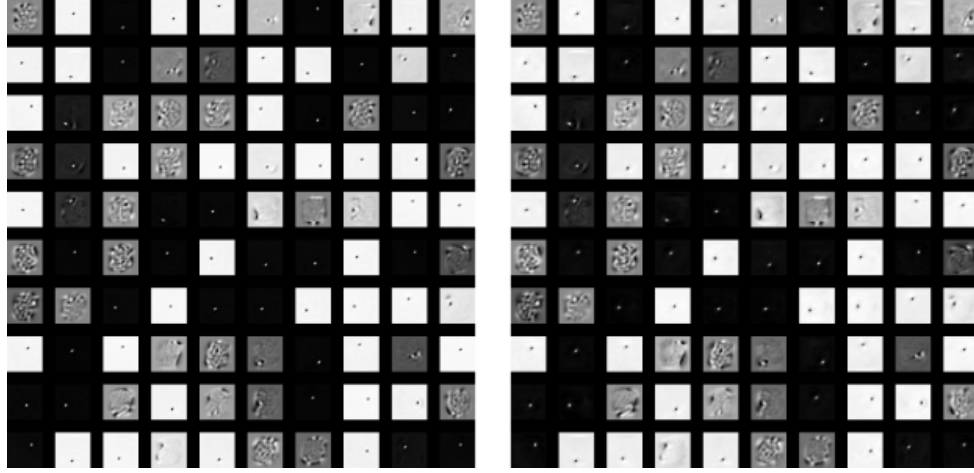


Figure 1: The weights of encoder  $W$  (Left) and weights of decoder  $R^T$  (Right) for a contractive auto-encoder trained with weight length constraints are shown.

One natural way to regularize the auto-encoder is to put a weight length constraints  $\|\mathbf{w}_i\|^2 \alpha_i$ . Typically, the weights grow very huge as the model fits the data, even with the weight decay cost. We impose length of weights to be fixed by relatively scaling down the weights. De facto, this naturally obtains weight-decay constraints and also possesses contractive property since contractive term (norm of jacobian matrix w.r.t hidden units) contains the term,  $\|W\|^2$ . Moreover, having a sufficient weight length size so that

Autoencoder	Relu	Relu+wl	sig.+wl	sig.+wl
AE	95.9%	98.7%	95.1%	99.1%
CAE	95.2%	98.6%	97.4%	99.1%

Figure 2: Symmetricity of ADW after training AEs with 500 units on MNIST for 100 epochs. We denote the auto-encoders with weight length constraints as 'wl'.

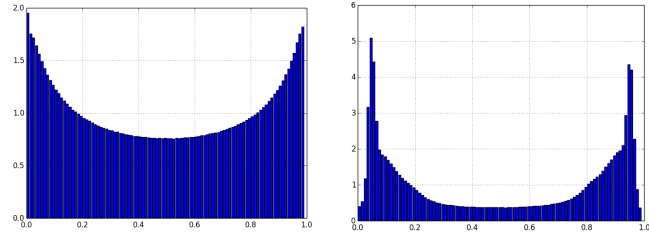


Figure 3: Histograms of hidden activations for sigmoid units without weight constraints (left) and with weight constraints (right)

Figure 2 demonstrates that weight length indeed helps  $\frac{\partial r(\mathbf{x})}{\partial \mathbf{x}}$  to be more symmetric. AE with weight length constraints denoted as "AE sig wl", gets symmetry score of 0.9914 and CAE with weight length constraints denoted as "CAE sig wl", gets symmetric score of 0.9916.

Furthermore, examining the weights of an encoder and decoder shows that the two weights are indistinguishable from one and other. Figure 1 presents the contractive auto-encoder trained with weight length constraints. The improvement in the symmetricity is clear when they are compared to Figure ???. When the regular auto-encoder is trained,  $R$  was smoothed version of  $W$ . However, we do not observe this in Figure 1. This implies that  $R$  is becoming like  $W$  when we straightly enforce  $\|W\| = \|R\|$ , which brings back to having a symmetric auto-encoder.

Based on above results, we see that our sufficient condition could explain the what is going on with filters for the auto-encoder with sigmoid activation. Moreover, having a weight length constraints,  $\|W\| = \|R\|$  leads to  $R \rightarrow W$ .

$$\sum_k h'(\mathbf{w}_k^T \mathbf{x}) \|\mathbf{w}_k\|^2 < D \quad (9)$$

will make the point  $\mathbf{x}$  to be sink of the auto-encoders dynamics is desirable condition.

Next, obvious question to ask is will deeper auto-encoders be symmetric as well? We plotted  $\frac{\partial r(\mathbf{x})}{\partial \mathbf{x}}$  for two hidden layer untied auto-encoders. Figure 4 illustrates that they have harder time becoming fully symmetric, but still desire for symmetricity.

Another way of explicitly measuring the conservativeness as the auto-encoder gets trained is to look at the curl. In our experiments, we created three 2D syntehtic datasets to understand the auto-encoder’s dynamics while learning. The three datasets consists of manifolds that looks like line, circle, and spiral. We looked at the changes in the vector field of before training, intermidate stage, and final stage. We also examined the magnitude of the curl and show that magnitude of curl decreases during the training. We also notice that sigmoid activation deforms the vector fields very slowly whereas, having relu acitvion function, changes the vector fields very rapidly. Figure 5, 6, and 7 shows the initial, final vector fields, and the magnitude of curl near the manifold. The color of vector field indicates the mean reconstruction error rates.

In fact, after conducting this experiments, we argue that studying the dynamics of vector field is a excellent way of understanding the changes in the enery surface during the training, because we get the idea of how energy surface deforms by observing the changes in the vector fields.

### 3 Computing the potential energy

In this section, we propose a way to compute the energy function for auto-encoders with untied weights for any activation function. A high level overview of our proposed method is to find an auto-encoder with tied weights that is equivalent to well-defined auto-encoder with untied weights at point  $\mathbf{x}$ . Note that the term “well-defined” is crucial to our assumption. The energy function in [1] applies to any auto-encoders with tied weight. On the contrary, what we meant by “well-defined” for untied auto-encoder is that they are trained to acquire symmetric matrix in  $\frac{\partial r(\mathbf{x})}{\partial \mathbf{x}}$  as described in Section ??.

When locally linearized auto-encoder satisfies Equation ?? so that it is symmetric, then we can also formulate it as

$$\frac{\partial r(\mathbf{x})}{\partial \mathbf{x}} = R\hat{W}^T = \hat{S}\hat{S}^T \quad (10)$$

where  $UDU^T$  is the eigen-decomposition of  $A\hat{W}^T$  and  $\hat{S} = UD^{\frac{1}{2}}$ .

Equation 10 implies that there exist an equivalent auto-encoder with tied weights  $\hat{S}$ . By letting

$$\mathbf{s}_k = \frac{\hat{\mathbf{s}}_k}{h'(\mathbf{s}_k^T \mathbf{x})^{\frac{1}{2}}}, \quad (11)$$

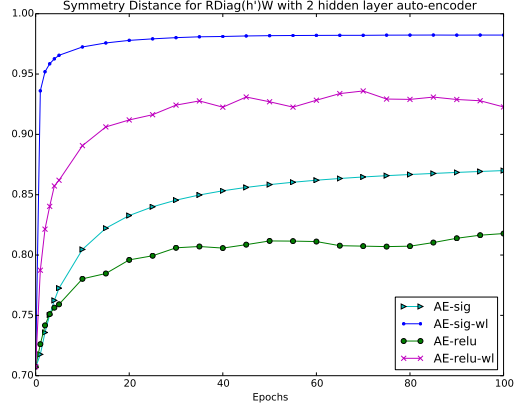


Figure 4: Figure presents symmetric distance of  $\frac{\partial r(\mathbf{x})}{\partial \mathbf{x}}$  for two hidden layer untied auto-encoder

we get an auto-encoder with tied weights  $S = \hat{S}/\text{diag}(h'(S\mathbf{x}))$ . We can verify that the two auto-encoders are the same by looking at their reconstruction function:

$$\begin{aligned}
r(\mathbf{x}) &= \int \frac{\partial r(\mathbf{x})}{\partial \mathbf{x}} d\mathbf{x} \\
&= \int R(\text{diag}(h'(W^T \mathbf{x}) W^T)) d\mathbf{x} \\
&= \int \hat{S} \hat{S}^T d\mathbf{x} \\
&= \int S \text{diag}(h'(S^T \mathbf{x})) S^T d\mathbf{x} \\
&= Sh(S^T \mathbf{x}) + \mathbf{c}'
\end{aligned} \tag{12}$$

where  $\mathbf{b}'$  and  $\mathbf{c}'$  are the constant term. **Dan: I am not sure what happens with constant. I think the constant terms are the same for all input.** We can also validate by deducing from  $r(\mathbf{x}) = Sh(S^T \mathbf{x}) + \mathbf{c}'$  to  $\frac{\partial r(\mathbf{x})}{\partial \mathbf{x}}$ . This confirms that  $r(\mathbf{x}) = Sh(S^T \mathbf{x}) + \mathbf{c}' = Rh(W^T \mathbf{x} + \mathbf{b}) + \mathbf{c}$ . Therefore, the potential energy of the auto-encoder with untied weights is the same as the auto-encoder with tied weight  $S$  at  $\mathbf{x}$  and it is given by

$$E(\mathbf{x}) = \int h(\mathbf{s}_k^T \mathbf{x}) d\mathbf{x} - \beta(\mathbf{x}). \tag{13}$$

where  $\beta(\mathbf{x}) = \frac{1}{2} \|\mathbf{x} - \mathbf{c}'\|_2^2 + \text{const}$ . In fact, by normalizing the data to be centered at zero, we can make  $\mathbf{c}'$  to be zero. Remark that finding a closed form solution to the implicit function in Equation 11 is not straight forward. In practice, we have to use iterative projection method to solve  $\mathbf{s}_k$ , and  $\mathbf{s}_k$  will be usually some local solution due to the non-convexity of Equation 11.

The same idea can be directly applied to piecewise linear auto-encoders like zero-biased auto-encoder [?] or auto-encoders with relu activation functions. The derivations for the potential energy for peicewise deep auto-encoder is provided in the supplementary material.

### 3.1 Computing the potential energy for piecewise linear auto-encoders

In this section, we propose a way to compute the energy function for auto-encoders with untied weights for piecewise linear auto-encoders. For example, rectified linear activation function is one of most popular activation function in neural network community and it is defined by

$$h(x) = \begin{cases} x & : x > 0 \\ 0 & : \text{Othewise} \end{cases}$$

They have been empirically demonstrated that learning of neural network performs faster and better than sigmoid functions due to the agility of gradients propagating over the whole network [?]. Also, it intrisically cheers sparsity in the activations of hidden units.

Let  $\gamma(\mathbf{x}) = \{k | h_k(\mathbf{x}) = \sum_i W_{ki} x_i > 0\}$  be the indices of active set for  $\mathbf{x}$ . Then the auto-encoder with rectified linear activation function can be written as

$$r_j(\mathbf{x}) = \sum_k^{\gamma(\mathbf{x})} R_{ij} \left( \sum_i W_{ki} x_i + b_k \right) + c_j. \tag{14}$$

To simplify this into a matrix form, we let  $\tilde{W} = W * \mathcal{I}(\gamma(\mathbf{x}))$  and  $\tilde{R} = (R^T * \mathcal{I}(\gamma(\mathbf{x})))^T$  where  $\mathcal{I}_i(\gamma) = \begin{cases} 1 & : \text{If } i \in \gamma(\mathbf{x}) \\ 0 & : \text{Othewise} \end{cases}$  is an indicator function, and similarly for the biases,  $\tilde{\mathbf{b}} = \mathbf{b} * \mathcal{I}(\gamma(\mathbf{x}))$ . Ergo, the auto-encoder merely becomes an affine auto-encoder such that

$$r(\mathbf{x}) = R(\tilde{W}^T \mathbf{x} + \tilde{\mathbf{b}}) + \mathbf{c} \tag{15}$$

and its derivative with respect to  $\mathbf{x}$  becomes

$$\frac{\partial r(\mathbf{x})}{\partial \mathbf{x}} = \tilde{R} \tilde{W}^T. \tag{16}$$

Following the same procedure in Section 3, we can use eigen decomposition to decompose  $\tilde{R}\tilde{W}^T$  into  $\hat{S}\hat{S}^T$ . Since  $\frac{\partial h(\mathbf{u})}{\partial \mathbf{u}} = I$  due to the linearity,  $\hat{S} = S = UD^{\frac{1}{2}}$ . Therefore, we found a shallow (1-layer) symmetric auto-encoder that has the energy function

$$E(\mathbf{x}) = \|S\mathbf{x} + \tilde{\mathbf{b}}\|_2^2 - \beta(\mathbf{x}) \quad (17)$$

and has the same energy at point  $\mathbf{x}$  as the original asymmetric auto-encoder. Note that as long as we can find an active set given a point  $\mathbf{x}$ , this generalizes to any piecewise linear activation function. For instance, the above applies to zero-bias auto-encoder when excluding the bias terms [?].

### 3.2 Computing the potential energy for piecewise Deep auto-encoders

The same idea of computation the potential energy can be directly applied to deeper layers of auto-encoders. Lets consider an auto-encoder with  $N$  layer encoder and  $N$  layer decoder such that

$$r(\mathbf{x}) = W^{2N}h\left(W^{2N-1}\dots h(W^{1^T}\mathbf{x} + \mathbf{b}^1)\right) + \mathbf{c}^N \quad (18)$$

where  $W^{N+i^T} = R^i \forall i = 1 \dots N$ . Then we can define an  $2N - 1$  number of active sets such that

$$\gamma^l(\mathbf{x}) = \left\{k|h_k^l(\mathbf{x}) = W^l h^{l-1}\left(W^{l-1} h^{l-2} \dots h^1(W^{1^T}\mathbf{x})\right) > 0\right\}.$$

where  $l$  is the index of each layer. We can rewrite in terms of matrix form as

$\tilde{W}^l = \left(W^{l^T} * \mathcal{I}(\gamma^{l-1}(\mathbf{x}))\right)^T * \mathcal{I}(\gamma^l(\mathbf{x}))$  and  $\tilde{\mathbf{b}}^l = \mathbf{b}^l * \mathcal{I}(\gamma^l(\mathbf{x}))$ . Hence, the auto-encoder can be linearized into

$$r(\mathbf{x}) = \tilde{W}^{2N}\left(\tilde{W}^{2N-1}\dots(\tilde{W}^{1^T}\mathbf{x} + \tilde{\mathbf{b}}^1)\right) + \tilde{\mathbf{b}}^{2N} \quad (19)$$

and its derivative with respect to  $\mathbf{x}$  becomes the product of weights:

$$\frac{\partial r(\mathbf{x})}{\partial \mathbf{x}} = \prod_{l=1}^{2N} \tilde{W}^l. \quad (20)$$

Assuming that  $\frac{\partial r(\mathbf{x})}{\partial \mathbf{x}}$  will endeavor for symmetry from training the deep auto-encoder, we can decompose this into symmetric matrices  $\frac{\partial r(\mathbf{x})}{\partial \mathbf{x}} = SS^T$ , again by applying eigen decomposition, where  $S = UD^{\frac{1}{2}}$ . Then, in the same manner as shallow (1-layer) symmetric auto-encoder, we can formulate the energy function as

$$E(\mathbf{x}) = \|S\mathbf{x} + \tilde{\mathbf{b}}\|_2^2 - \beta(\mathbf{x}). \quad (21)$$

## 4 Approximating the energy function

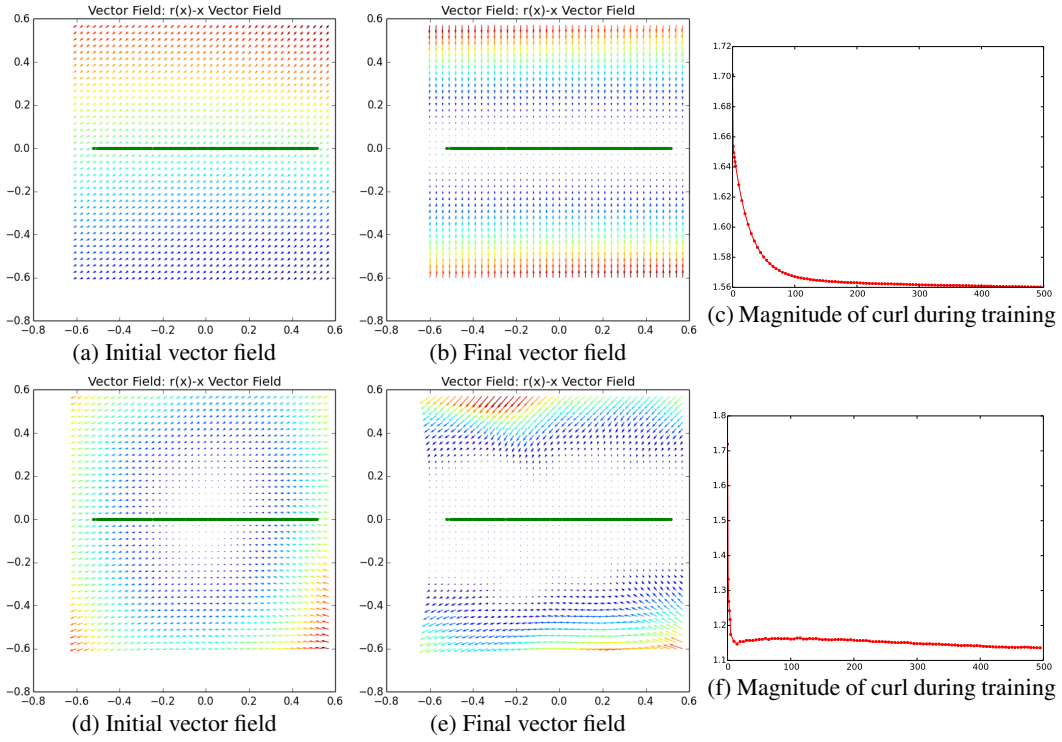


Figure 5: Initial and final vector field after training untied auto-encoder on line dataset.

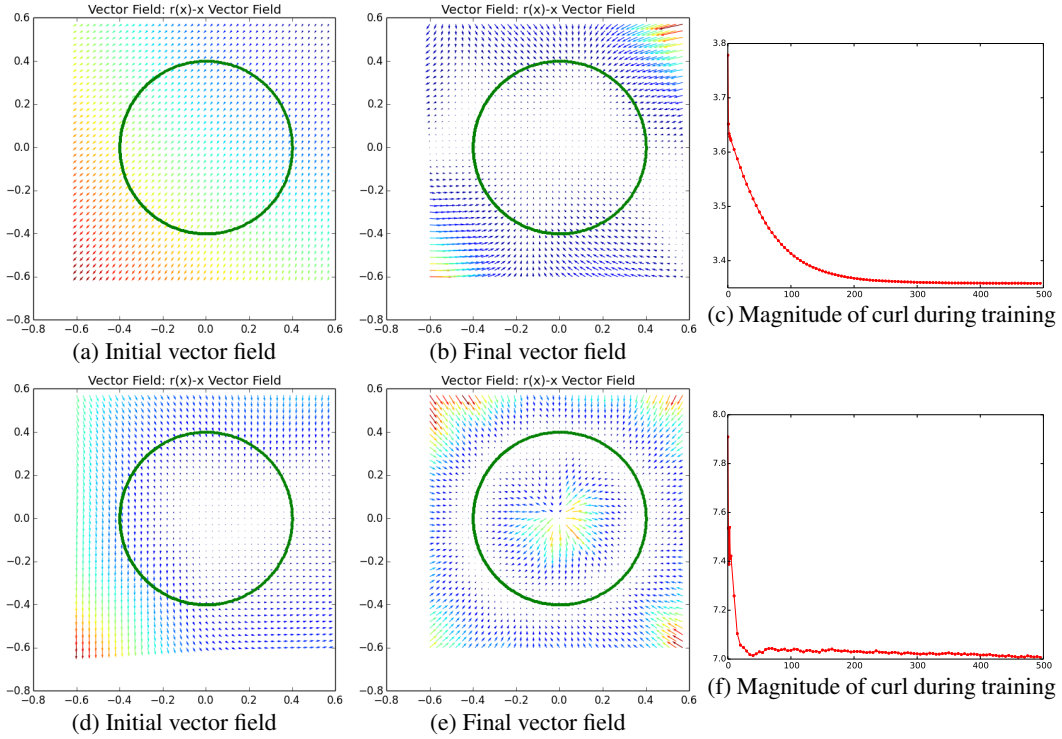


Figure 6: Initial and final vector field after training untied auto-encoder on circle dataset.

## References

- [1] Hanna Kamyshanska. On autoencoder scoring. In *Proceedings of the International Conference on Machine Learning (ICML)*, pages 720–728, 2013.



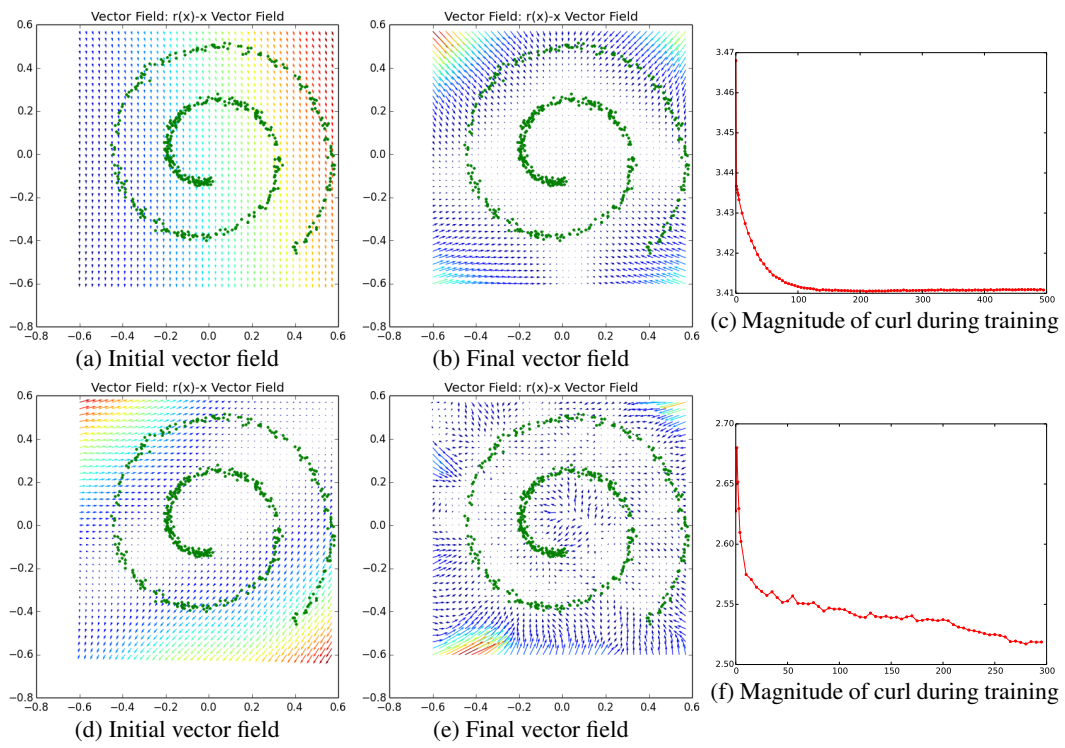


Figure 7: Initial and final vector field after training untied auto-encoder on spiral dataset.